XIII ICSMFE, 1994, New Delhi, India / XIII CIMSTF, 1994, New Delhi, Inde

ON THE SCALE EFFECT OF FOOTINGS ON SAND UNDER GENERAL LOADS

L'EFFET D'ECHELLE DE SEMELLES SUR SABLE SOUS CONDITIONS GENERALES DE CHARGEMENT

G. Gottardi[1] **G. Ricceri**[2] **P. Simonini**[3]

[1]University of Padova, Italy
[2]Professor of Soil Mechanics, University of Padova, Italy
[3]Researcher, University of Padova, Italy

SYNOPSIS

The influence of the scale effect on the behaviour of surface footings on sand subjected to general loading conditions is analysed in the paper. The problem is investigated using two different approaches. The former, experimental, considers the results obtained from bearing capacity tests performed on foundations of different widths using a large three-dimensional small scale physical model, recently built at the University of Padova. The latter is an analytical approach, based on the kinematic method of limit analysis and applied to a rigid block failure mechanism in which the non-linear strength envelope of sand is taken into account. The results of experimental and analytical studies are compared in terms of dimensionless interaction diagrams of the applied loading components.

INTRODUCTION

The bearing capacity of surface footings subjected to general loading conditions is usually calculated according to Brinch-Hansen's (1970) well-known extension of the Terzaghi formula, in which inclination α and eccentricity e of the resultant external load are taken into account by means of linear superposition of numerous and empirical correction factors. In the simple case of a strip surface footing resting on a horizontal and homogeneous layer of dense sand, that expression becomes:

$$q_l = 1/2 \ \gamma \ B \ N_\gamma \ i_\gamma \ e_\gamma \qquad (1)$$

where:
- q_l is the vertical component of limit pressure;
- γ is the unit weight of sand;
- B is the footing breadth;
- N_γ is the bearing capacity factor;
- i_γ and e_γ are load inclination and eccentricity factors.

The most common expressions of i_γ are those proposed by Meyerhof (1963) and Brinch-Hansen (1970), while Meyerhof's (1953) equivalent-breadth concept is widely used when the load is eccentric.

Bearing capacity analysis can be alternatively carried out through the introduction of interaction diagrams relating to the different loading components at failure (Butterfield & Ticof, 1979). For the planar case of a strip footing, we can define a surface in the loading components space V-H-M/B (V is the vertical load, H is the horizontal load and M/B is the overturning moment divided by the footing breadth for dimensional homogeneity) inside which all allowable loading combinations must lie.

The form of the complete non-symmetrical surface has been recently established (Gottardi, 1992), but the parabolic shape of its projection on V-H and V-M/B planes has been experimentally confirmed by several authors (Ticof, 1977; Georgiadis & Butterfield, 1988; Montrasio & Nova, 1988; Ricceri & Simonini, 1989). On the other hand, plotted in this way, classic expressions of i_γ and e_γ provide a similar trend.

Interaction diagrams are generally plotted in dimensionless form, the loading components being normalised to the ultimate vertical central load V_{max}. However, since they are obtained as failure envelope of load tests on small scale physical models, we have to take into account the possible influence of scale effect on experimental data.

Scale effect on the bearing capacity of surface footings has been well established among geotechnical researchers for a long time. DeBeer (1965) was the first to propose two main reasons as an explanation for the decreasing of N_γ with footing breadth B, i.e. the variation of friction angle ϕ' with effective pressure level and the progressive failure which produces the so-called "particle size effect".

Even if an analysis based on the stress dependency of ϕ' only (Hettler & Gudehus, 1988) appears to provide results that correspond to experimental data, discussion about the relative importance of the two above factors is still in progress (Tatsuoka et al., 1989), making large use of results from loading tests in centrifuge which is particularly suitable for investigating this subject (Kusakabe et al., 1991).

This paper intends to investigate whether dimensionless expressions of interaction diagrams in V/V_{max}-H/V_{max} and V/V_{max}-M/BV_{max} planes depend on footing width or, in the same way, whether factors i_γ and e_γ are influenced also by scale effect.

Following a well-developed research project, a new experimental programme was carried out using a large three-dimensional model. Even if the accurate control of parameters and the precise measurement of data allow for a reliable comparison of loading test results, the range of footing widths which can be investigated is rather limited. Therefore a simple but powerful theoretical model, based on the kinematic method of limit analysis and incorporating variations of ϕ' along failure surfaces, was also developed in order to extend results to full size foundations.

CHARACTERISTICS OF FOUNDATION SAND

The soil used in the model tests carried out is a medium-fine uniform sand coming from the mouth of Adige River, Italy, whose characteristic values are: mean particle size D_{50} = 0.42 mm; uniformity coefficient C_U = 2.04; unit weight of solid particles 26.6 kN/m³; minimum and maximum dry unit weights 13.58 and 16.51 kN/m³. The dependence of friction angle on pressure level is interpreted using a power relationship (Hettler and Gudehus, 1988) fitting the results of isotropic triaxial compression tests, performed on samples reconstructed approximately at the same density of

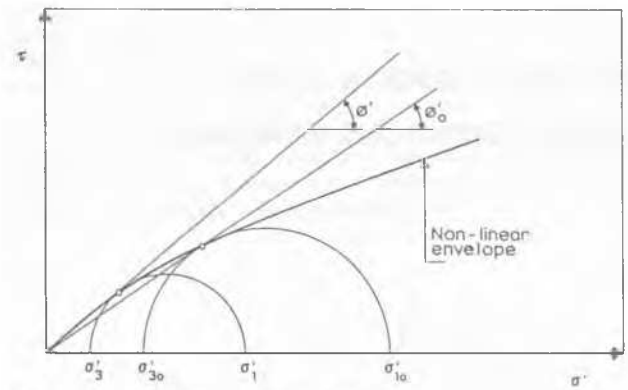

Fig. 1. Non-linear strength envelope of sand

foundation beds and with confining pressures in the range 30-2000 KPa (Ricceri and Simonini, 1991).
According to Hettler and Gudehus the secant angle ϕ' is given by the following relationship (figure 1):

$$\phi' = \frac{\sin\phi'_o}{(\sigma'_1/\sigma'_{3o})^{\beta} + \sin\phi'_o[1 - (\sigma'_1/\sigma'_3)^{\beta}]}, \qquad (2)$$

where $\phi'_o = 40.5°$ for $\sigma'_3 = 196.2$ KPa. The curvature parameter ß is estimated at 0.11. Note that the friction angle varies from 44.2° to 35.7° in the range of confining pressures investigated.

MODEL TESTS

The experimental apparatus used for bearing capacity tests is a large physical model which was developed at the University of Padova (Ricceri & Simonini, 1989) and then improved in order to submit the footing plate to any allowable load-path (Gottardi, 1992).
The model essentially consists of a fixed test tank (1800x1800x600 mm) which is gradually filled with sand by controlled pluvial deposition. All mechanisms are fully automatic and allow for the achievement of essentially homogeneous and highly reproducible foundation beds, the standard deviation of the relative density measured throughout identical tests being less than 1% (Gottardi, 1992).

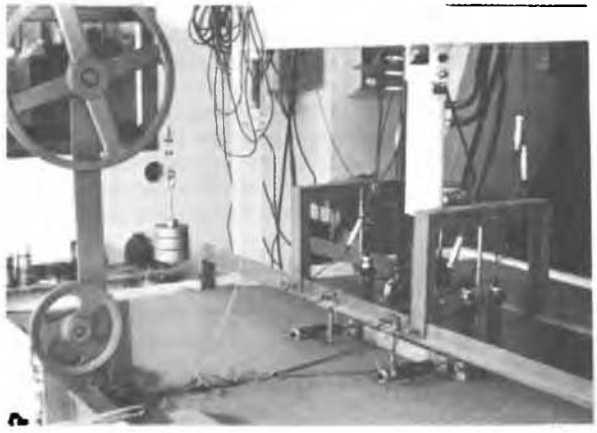

Fig. 2. View of the experimental set up

The loading device comprises an arch which supports a servo-controlled hydraulic jack and can be moved to provide any load inclination at a range of eccentricities determined by grooves spaced along the footing. A novel device has also been developed in order to apply horizontal loads precisely at the base of the footing and independently of the jack (figure 2). Both loading devices are provided with high precision strain-gauged load cells and all data recorded on a programmable logger.
To ensure a fully rough soil-foundation contact, Adige sand was glued to the bottom surface of all footing plates. The load was applied in fixed small steps, up to failure conditions which always occurred suddenly after the peak strength had been exceeded. A high value of relative density (85%) was in fact selected for all foundation beds in order to ensure that general failure developed within the soil.
Three steel U-section rigid plates - whose dimensions are shown in table 1 - were used, according to the requirement that slip surfaces could not interact with tank walls. Each footing was submitted to 7 different bearing capacity tests (summarised in table 2), the loading path being the only variable parameter.
The fundamental reference test, vertical central load (V-C), provides the ultimate value V_{max} for each footing. Inclined, central loads increasing monotonically (I-C) are represented in V-H plane by "radial" load-paths (in figures 3 and 4 only load-paths of footing B are plotted). The same trend in V-M/B plane shows load-paths of vertical, eccentric load tests (V-E). Two more tests in V-H plane, in which ΔV increments were applied initially, followed by ΔH increments to failure at V/V_{max} = constant, are represented by "right-angled" load-paths (V-H).

Table 1. Characteristics of footing plates

Footing	B (mm)	L (mm)	L/B	N_γ
A	50	250	5	494
B	100	500	5	401
C	140	700	5	332

Table 2. Summary of bearing capacity tests

Test No.	Load-Path	α (°)	e/B	V/V_{max}
1	V-C	0.0	0.0	-
2	I-C	5.0	0.0	-
3	I-C	12.5	0.0	-
4	V-E	0.0	1/10	-
5	V-E	0.0	1/6	-
6	V-H	-	-	0.50
7	V-H	-	-	0.75

TEST RESULTS ANALYSIS

Bearing capacity factor N_γ, back-calculated with (1) from V-C tests (table 1), shows, as expected, a marked scale effect. Even within the narrow range of footing widths investigated, we can clearly observe a sharp decrease of dimensionless bearing capacity.
It is interesting to point out whether interaction diagrams, in which loading components are normalised with respect to V_{max}, are similarly affected by such a scale effect.
In figure 3 the points representing failure loads for all tests with negligible moment component are plotted and compared between two interaction diagrams: the dotted line is derived from Brinch-Hansen's expression of i_γ, the solid line is an interpolation curve - a very simple, symmetric, second-order parabola - obtained on the basis of a lot of other data from the same model and B = 100 mm (Gottardi, 1992). These points, of course, turn

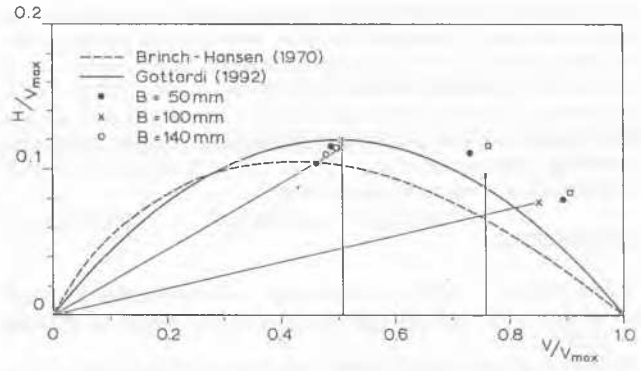

Fig. 3. Experimental results in the V/V_{max}-H/V_{max} plane

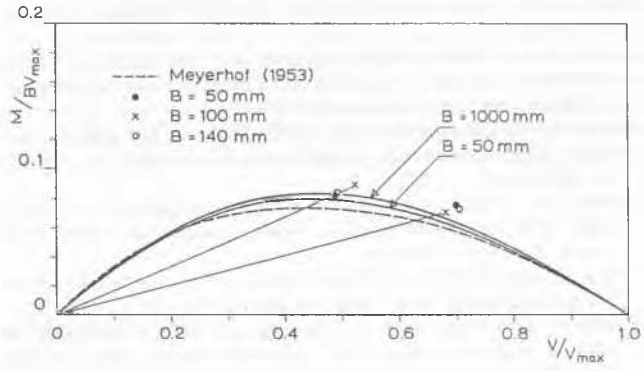

Fig. 4. Experimental and analytical results in the V/V_{max}-M/BV_{max} plane

out to be grouped according to the load-path followed to achieve failure, but no appreciable influence of footing width can be singled out, at least within experimental approximation. The more variable failure loads on the descending side of the parabola may be justified by higher stress levels and increased vertical displacements. Note that errors are nevertheless on the "safe side" with respect to above mentioned interaction diagrams. When $V/V_{max} \approx 0.50$, on the contrary, all failure points lie in a very limited region of the diagram, irrespectively of loading path and footing width.

Brinch-Hansen's factor seems to provide more conservative values, except in the initial part, when V/V_{max} approaches zero and where the tangential slope at the origin, instead of being 45°, should rather equal δ (δ being the soil-footing interface friction angle).

In V/V_{max}-M/BV_{max} plane (figure 4) fewer points are available (with described apparatus it is not possible to apply $\Delta M/B$ increments only), but again no remarkable scale effect appears to influence experimental data. Meyerhof's equivalent-breadth concept, plotted this way, goes to provide very precise bearing capacity predictions, even if a little too conservative. The two other curves which appear in figure 4 are calculated by means of the kinematic model described below.

KINEMATIC ANALYSIS

The kinematic approach of limit analysis is a powerful and rigorous tool in solving limit equilibrium problems in soil mechanics (Chen, 1975). For its application to the bearing capacity evaluation of surface footings, the development of general shear failure, characterised by well defined sliding surfaces, is required. Thus, the soil deformation mode can be interpreted in terms of sliding blocks, satisfying velocity boundary conditions, strain and velocity compatibility conditions.

The failure mechanism selected to study the bearing capacity of surface footings of breadth B subjected to general loads is shown in figure 5. Such a mechanism consists of 6 blocks which are defined on the basis of angles α_i and β_i and sides a_i and b_i. The effect of eccentricity is taken into account by using the concept of Meyerhof's reduced width $B'=B-2e$.

The curvature of strength envelope is introduced in the failure mechanism by permitting a discrete variation of the friction angle ϕ' along the external sliding surface Σa_i. A value of ϕ'_i corresponds to each segment a_i of the failure surface (figure 5).

In case of inclined load the external work is given by:

$$W_{ext} = qBV_o[1+\tan\alpha/\tan(\alpha_1-\phi'_1)], \qquad (3)$$

with V_o=vertical velocity of external load, and the internal rate of dissipation by:

$$W_{int} = \sum_{i=1}^{6} \gamma A_i V_i \cos\Theta_i , \qquad (4)$$

where Θ_i are the angles between vectors representing the weight of blocks (γA_i) and vectors of the corresponding velocities V_i.

In case of eccentric load B' is introduced in eq. (3).

The kinematic theorem affirms that the load q determined by equating the external work to the internal rate of dissipation in an assumed velocity field

$$q = 1/2\ \gamma B f(\alpha, \alpha_1,\beta_1,\phi'_1,\ldots\alpha_6,\beta_6,\phi'_6) \qquad (5)$$

is not less than the actual collapse load. In eq. (5) f is a function which summarises the contribution of each single block.

Since friction angles ϕ'_i are material parameters the solution of eq. (5) requires the minimisation with respect to α_i and β_i. Numerical minimisation is performed with the following limits on the variables:

$$\phi'_1 \le \alpha_1 \le \pi/4+\phi'_1/2; \quad \alpha_i \le \alpha_{i-1}+\beta_{i-1}; \quad \alpha_i < \pi-\beta_i.$$

The minimum value of f is the well-known bearing capacity factor which, in this case, directly incorporates the effect of load inclination.

In order to take into account the variation of friction angle with the pressure level in each discontinuity of the mechanism, a simplified normal

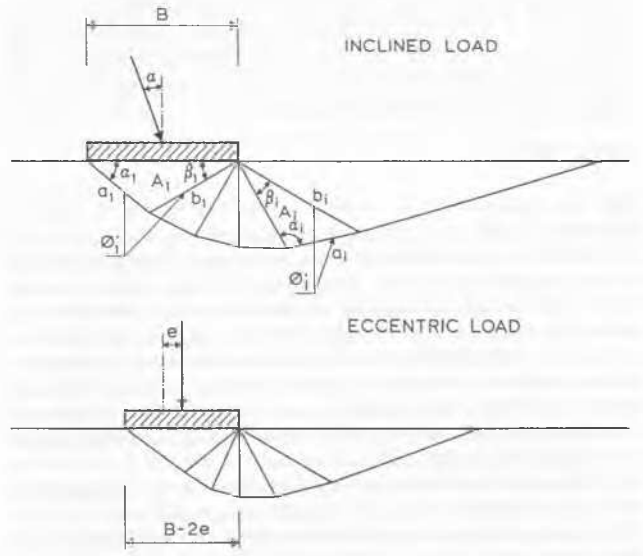

Fig. 5. Kinematic mechanisms for inclined and eccentric load

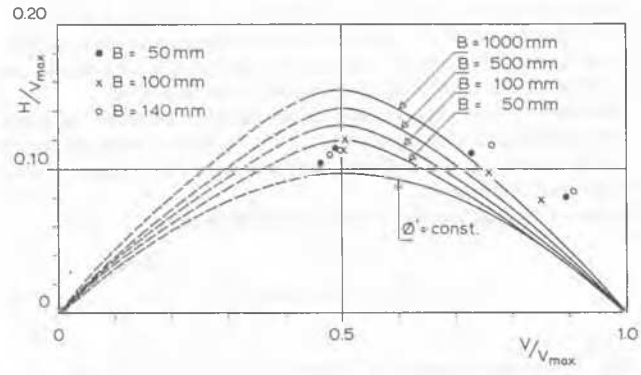

Fig. 6. Experimental and analytical results in the V/V_{max}-H/V_{max} plane

stress distribution acting along the failure surfaces together with eq. (5) is used. The solution is obtained by an iterative numerical technique searching the minimum equilibrium condition of the block mechanism (Ricceri and Simonini, 1991).
Different load inclinations and eccentricities were considered in the bearing capacity analysis of 4 footing widths (B=50, 100, 500, 1000 mm).

EXPERIMENTAL VS. ANALYTICAL RESULTS

The results of kinematic analyses are plotted in terms of interaction diagrams for inclined (figure 6) and eccentric (figure 4) load.
The left side of the envelopes in the diagram of figure 6 is only hypothesised and thus plotted with a dashed line. In fact, at lower vertical loads, a different mechanism of failure takes places characterised by sliding on the horizontal plane. On the same graph the interaction diagram calculated by assuming a constant value of ϕ' in the whole mechanism is also drawn.
A small scale effect on bearing capacity can be appreciated by considering the analytical envelopes for different widths: the larger the footing width, the higher the maximum horizontal load. Close agreement with experimental data can be observed for $V/V_{max} \approx 0.5$. Note that the constant friction angle envelope represents a lower limit with respect to experimental data and also to other analytical results.
On the contrary, the envelopes in the V/V_{max}-M/BV_{max} plane (figure 4) show a negligible scale effect. Thus only the extreme curves, i.e. for B = 50 mm and B = 1000 mm, are reported. Note that Meyerhof's envelope corresponds to ϕ'=constant-condition in the kinematic mechanism. It can be observed that experimental results are closer to the analytical envelopes obtained in the case of variable friction angle.

CONCLUSIONS

From the experimental and analytical modelling carried out at the University of Padova the following conclusions can be drawn:
1. The presence of a marked scale effect on the bearing capacity of surface footings on sand is confirmed. Even within the small range of footing widths experimentally investigated, a sharp decrease of the self-weight bearing factor is observed when the applied load is vertical and central.
2. The use of dimensionless interaction diagrams of loading components can be considered a simple but powerful tool in predicting the actual bearing capacity of surface footings under general loads. Their shape, based on experimental data, can be expressed by a second-order parabola in the case of both inclined and eccentric load.
3. No evident scale effect can be appreciated on the dimensionless interaction diagrams determined on the basis of 1-g model tests.
4. The theoretical analyses are performed using a kinematic mechanism of failure, which allows for a variation of friction angle with a stress level along the sliding surface. They show that increasing the width of the footing, maximum dimensionless horizontal load or moment are also slightly increased. This scale effect, more appreciable for footing subjected to inclined loads, can be partially explained by taking into account the curvature of the strength envelope of dense sand.
5. Anyway, comparing the results of model tests and kinematic analyses, the dimensionless interaction diagrams determined by small scale physical modelling appear to provide a safe estimate of the ultimate load of full scale surface footings under general loads.

REFERENCES

Brinch-Hansen, J. (1970): A revised and extended formula for bearing capacity. *Bull. n.98, The Danish Geotechnical Institute*, Copenhagen, pp.5-11.

Butterfield, R. and Ticof, J. (1979): The use of physical models in design. Discussion. *Proc. VII European Conf. Soil Mech. Found. Eng.*, Brighton, Vol.4, pp.259-261.

Chen, W.F. (1975): *Limit Analysis and Soil Plasticity*. Elsevier, Amsterdam.

DeBeer, E.E. (1965): Bearing capacity and settlement of shallow foundations on sand. *Proc. Symp. on Bearing capacity and settlement of foundations*, Duke University, pp.15-33.

Georgiadis, M. and Butterfield, R. (1988): Displacements of footings on sand under eccentric and inclined loads. *Can. Geotech. Jl.*, Vol.25, pp.199-212.

Gottardi, G. (1992): Modellazione del comportamento di fondazioni superficiali su sabbia soggette a diverse condizioni di carico. *Ph.D. thesis*, University of Padova.

Hettler, A. and Gudehus, G. (1988): Influence of the foundation width on the bearing capacity factor. *Soils and Foundations*, Vol.28, pp.81-92.

Kusakabe, O., Yamaguchi, H. and Morikage, A. (1991): Experiment and analysis on the scale effect of N_γ for circular and rectangular footings. *Centrifuge 91*, Balkema, Rotterdam, pp.179-186.

Meyerhof, G.G. (1953): The bearing capacity of foundations under eccentric and inclined loads. *Proc. Third Int. Conf. Soil Mech. Found. Eng.*, Zurich, Vol.1, pp.440-445.

Meyerhof, G.G. (1963): Some recent research on the bearing capacity of foundations. *Can. Geotech. Jl.*, Vol.1, pp.16-26.

Montrasio, L. and Nova, R. (1988): Assestamenti di una fondazione modello sotto carico inclinato: risultati sperimentali e modellazione matematica. *Riv. It. Geot.*, Vol.22, pp.35-49.

Ricceri, G. and Simonini, P. (1989): Interaction diagrams for shallow footings on sand. *Proc. XII Int. Conf. Soil Mech. Found. Eng.*, Rio de Janeiro, Vol.2, pp.967-972.

Ricceri, G. and Simonini, P. (1991): Curvatura dell'inviluppo a rottura e capacità portante di fondazioni superficiali in terreni granulari. *Riv. It. Geot.*, Vol.25, pp.49-62.

Tatsuoka, F., Tani, K., Okahara, M., Morimoto, T., Tatsuta, M., Takagi, S. and Mori, H. (1989): Influence of the foundation width on the bearing capacity factor. Discussion. *Soils and Foundations*, Vol.29, pp.146-154.

Ticof, J. (1977): Surface footings on sand under general planar loads. *Ph.D. thesis*, University of Southampton.